QUANTUM YIELD AND IMAGE CONTRAST OF BACTERIOCHLOROPHYLL MONOLAYERS IN PHOTOELECTRON MICROSCOPY

ROBERT B. BARNES, JULIANNE AMEND, WILLIAM R. SISTROM, AND O. HAYES GRIFFITH, *Institute of Molecular Biology and the Departments of Chemistry and Biology, University of Oregon, Eugene, Oregon 97403 U.S.A.*

ABSTRACT The photoelectron quantum yield spectrum of bacteriochlorophyll a_{Gg} (Bchl *a*) from *Rhodospirillum rubrum* was determined in order to evaluate the possibility of mapping photoreceptor distribution and organization in bacterial chromatophores. The quantum yield is on the order of 1×10^{-3} electrons/incident photon at 180 nm and decreases to 2.5×10^{-5} electrons/incident photon at 230 nm. Photoelectron micrographs confirm the high contrast predicted between monolayers of Bchl *a* against a lipid background (calcium arachidate). A significant contrast difference is found between the two monolayer orientations, demonstrating that photoelectron microscopy is a sensitive detector of asymmetry in Bchl *a* monolayers.

INTRODUCTION

Recently the absolute photoelectron quantum yield spectra of the plant chlorophylls were determined (Dam *et al.*, 1975). The yields are about 100 times greater in the 180–240-nm wavelength band than the photoelectron quantum yield of typical lipid and protein components of biological membranes. This difference suggests the possibility of using photoelectron microscopy to map the positions and organization of photoreceptors in membranes. In photoelectron microscopy, the sample is irradiated with ultraviolet light and the resulting photoionized electrons that escape from the surface are accelerated and imaged on a phosphor screen. Contrast in the final image is determined by the photoelectron quantum yields rather than by electron scattering as in transmission or scanning electron microscopy. In this study, we extend these measurements to Bchl *a* from the purple photosynthetic bacteria, *Rhodospirillum rubrum* (Fig. 1). Since the chlorophyll is organized in photosynthetic membranes that are quite thin (i.e., < 100 Å) compared to the samples used in a conventional photoelectron quantum yield spectrum, we also examine defined monolayers of Bchl *a*.

MATERIALS AND METHODS

Preparation of Bchl a

Strain G-9 of *Rhodospirillum rubrum* was grown in the medium of Griffiths and Stanier (1956) at 34°C. This strain differs from the wild type in that it lacks colored carotenoids

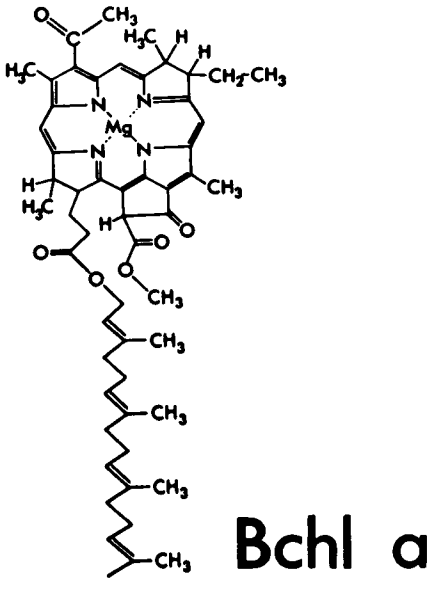

FIGURE 1

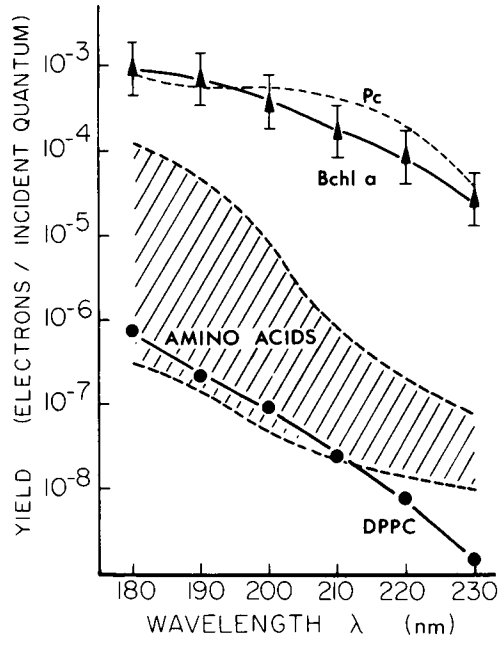

FIGURE 2

FIGURE 1 The structure of bacteriochlorophyll a_{Gg}.

FIGURE 2 The photoelectron quantum yield spectrum of Bchl *a* from *Rhodospirillum rubrum*. The dashed line is the reference quantum yield curve of metal-free phthalocyanine. The quantum yield curve of L-α-dipalmitoylphosphatidylcholine (DPPC) and the band of quantum yields of the common amino acids are also shown.

and is sensitive to photo-oxidation. To insure anaerobic conditions and to prevent photo-oxidation, a 5% CO_2 – 95% N_2 gas mixture was bubbled through the medium before and during illumination (tungsten lamp, 600 foot-candles). After being harvested by centrifugation, the cells were washed twice with distilled water. Extraction by methanol, separation by petroleum ether, and sucrose column chromatography were carried out by standard procedures (Holt and Jacobs, 1954; Sistrom, 1966). All steps were carried out under a green safelight.

The chromatographed Bchl *a* was identified by its characteristic optical spectra (Table I). The spectra exhibit the characteristic shift to longer wavelengths with increasing solvent polarity. Relative peak heights in all three solvents are in good agreement with literature values (Holt and Jacobs, 1954; Sistrom, 1966; Kim, 1966). The molar absorption coefficient at 770 nm was 95.8 $cm^2\ mmol^{-1}$, based on Bchl *a* molecular weight of 911.5. This agrees well with other published values (Holt and Jacobs, 1954; Weigl, 1953; and Kim, 1966). We conclude that our product is relatively pure Bchl *a*.

Monolayer Technique

The monolayer deposition process was performed by standard techniques (Blodgett, 1935; Sperling and Bacon, 1966). A circular glass container, cleaned in 3 N HCl, 3% H_2O_2, and then coated with paraffin, served as the subphase container. Compression was achieved through manual manipulation of a sliding Teflon-coated bar, and monitored by displacement

of a platinum foil Wilhelmy plate. Subphase water was in each case glass-redistilled. Calcium arachidate monolayers were formed on a subphase that consisted of 10^{-4} M recrystallized $CaCl_2$ in water buffered with 10^{-4} M Tris and adjusted to a pH of 8.0 with HCl. Arachidic acid (Sigma Chemical Co., St. Louis, Mo.), recrystallized three times from ethanol (mp 75°C), was dissolved in 15% benzene—85% *n*-hexane to a concentration of 7 mM. After the monolayer had spread, it was compressed to 30 dyn/cm. Bchl *a* monolayers were formed on the same subphase, but without the inclusion of $CaCl_2$. The subphase was cooled to 15°C by an ice bath. Bchl *a* was dissolved in 15% benezene–85% *n*-hexane to a concentration of 2×10^{-4} M. After the monolayers had spread, they were compressed to 15–25 dyn/cm. All of the above procedures were carried out under subdued green light.

For the quantum yield measurements the monolayers were deposited on the ends of carbon-coated stainless steel sample rods of 6.3 mm diameter. Multilayers of Bchl *a* were prepared in a number of ways. In one procedure carbon-coated sample rods were coated with 10–15 monolayers of calcium arachidate to form a low quantum yield substrate on a nonreflecting surface. Then 5–11 successive monolayers of Bchl *a* were deposited by repeated dipping of the sample rods, with the final layer oriented with the tetrapyrrole groups exposed at the air-sample interface (heads-up orientation). In another series of experiments, the arachidic acid coating was omitted. A third procedure consisted of depositing a thick coating of Bchl *a* onto carbon-coated sample rods by solvent evaporation from *n*-hexane. All of these procedures gave quantum yields within the experimental error bars of Fig. 2.

To prepare samples for photoelectron microscopy, two layers of calcium arachidate were deposited on a 5.0-mm diameter sample rod and dried for 5 min at 80°C. The first layer was heads down and the exposed layer was heads up. The coated sample rod was immersed so that the sample face was halfway submerged in the aqueous subphase. Then the Bchl *a* solution was spread under subdued light and compressed to 15 dyn/cm. The sample rod was withdrawn, coating one-half of the sample surface with a heads-down Bchl *a* monolayer. Heads-up Bchl *a* monolayers were formed under the same conditions in the following manner. Three monolayers of calcium arachidate were deposited on a carbon-coated sample rod and

TABLE I

OPTICAL ABSORBANCE OF BACTERIOCHLOROPHYLL *a*

Solvent	Peak wavelength	Relative absorbancy*			
		This work‡	Literature values§		
			a	b	c
	nm				
Methanol	771–772	100	100	—	—
	606–608	30.4	29	—	—
	366	107	106	—	—
Ethyl ether	770–771	100	—	100	100
	573–575	21.6	—	22.2	22.5
	391–392	52	—	49.9	58.4
	357–358	76.6	—	75.8	76.1
Chloroform	778–780	100	100	100	—
	582	26.4	28	28	—
	363	82.8	81	81	—

*Absorbancies are relative to that of the longest wavelength absorption maximum.

‡Estimated error ± 0.2.

§Literature references: a. Holt and Jacobs, 1954, b. Sistrom, 1966, c. Kim, 1966.

dried for 5 min at 80°C (final layer of arachidate was heads down). The rod was then lowered through a spread Bchl *a* monolayer. While the sample rod remained in the subphase, the surface was swept clean with lint-free lens paper, followed by further sweeping with a clean glass rod. The sample rod was then removed from the subphase.

Instrumentation

Photoelectron quantum yields were obtained in an ultrahigh vacuum stainless steel instrument and referenced to metal-free phthalocyanine described previously (Dam, et al., 1974*a*). Photoelectron micrographs were recorded in an ultrahigh vacuum photoelectron microscope (Dam and Griffith, 1976) utilizing three electrostatic lenses (E-Scope Inc., Cornelius, Ore.) The microscope is equipped with a 200-W cadmium-doped xenon arc lamp which exhibits several intense lines in the 200–240-nm region. These are the lines primarily responsible for the photoemission, although since no filter was used, longer wavelength light did reach the sample surface (i.e., the bandpass was limited only by the quartz optics transmission).

RESULTS AND DISCUSSION

The absolute photoelectron quantum yield is defined as the number of electrons released from the surface per incident photon. It does not correlate in any obvious way with the more familiar fluorescence quantum yield and the term quantum yield will be used throughout this paper to refer to the photoelectric measurement. The quantum yield of Bchl *a* over the wavelength range 180–230 nm is shown in Fig. 2. The dashed line is the quantum yield spectrum of the reference dye, metal-free phthalocyanine, Pc(Schechtman, 1968). Among the organic dyes examined so far, Pc exhibits one of the highest quantum yield curves, so it is apparent from Fig. 2 that Bchl *a* is also very photoemissive in this wavelength range.

The quantum yield spectrum of Bchl *a* is almost indistinguishable from that of plant chlorophyll *a* (Chl *a*), studied previously (Dam et al., 1975). The structure of Bchl *a* (Fig. 1) differs from Chl *a* in that ring II is reduced (additional H atoms at the 3 and 4 positions), an acetyl group replaces the ethylene side chain at the 2 position in ring I, and the 20-carbon geranylgeraniol hydrocarbon tail contains 3 more double bonds than does the phytol group of Chl *a* (Katz et al., 1972, Vernon and Seeley, 1966). These structural changes cause shifts in the visible and near infrared absorption maxima, but they evidently do not alter the conjugated tetrapyrrole nucleus sufficiently to change the quantum yield spectra in the wavelength region of Fig. 2.

For comparison, Fig. 2 also shows the quantum yield spectra of a typical phospholipid L-α-dipalmitoylphosphatidylcholine (DPPC, Griffith and Dam, 1976) and the band of quantum yields of the common amino acids (Dam et al., 1974*a*). All proteins without prosthetic groups should lie within this band because of the approximate additivity of the photoelectric effect. For example, the quantum yield spectra of apohemoglobin (Dam et al., 1974*b*) and bovine serum albumin (Griffith and Kongslie, unpublished data) do fall within this band. At wavelengths longer than 230 nm, all of the quantum yield curves of Fig. 2 continue to decrease monotonically until they drop below the limits of detection. At wavelengths shorter than 180 nm, the quantum yields increase and converge, minimizing the contrast. In the wavelength region 200–

230 nm, the Bchl *a* curve is two orders of magnitude greater than typical nonpigmented membrane components (Fig. 2). Consequently, this is the most favorable region for photoelectron microscopy.

A typical photoelectron micrograph of one monolayer of Bchl *a* is shown in Fig. 3. The bright areas result from electrons photoionized from Bchl *a* by the ultraviolet light. Only about one-half of the sample support is coated with Bchl *a* to show the contrast with the background surface of calcium arachidate. Small holes in the Bchl *a* monolayer are easily seen. The contrast is remarkable, considering that the sample is only one molecule thick.

The monolayer of Fig. 3 is oriented with the tetrapyrrole nuclei against the substrate (heads-down orientation). The photoelectron image of the heads-up monolayer is similar but is about three times brighter and corresponds to over half of the brightness of the thick Bchl *a* sample used to obtain the quantum yield curve. To interpret the image brightness quantitatively, it is useful to consider a four-step mechanism for photoemission: (*a*) absorption of the incident photons of energy $h\nu$ by molecules at depth r from the surface; (*b*) photoionization of molecules at depth r; (*c*) transport of the photoelectrons to the surface; and (*d*) escape from the surface into the vacuum. The yield Y_d for a sample of total thickness d is found by integrating the product of probabilities of the separate steps in photoemission and results in the well-known exponential relation (Spicer, 1972; Burke et al., 1974)

$$Y_d = Y[1 - e^{-d/d_0}], \tag{1}$$

where

$$d_0 = (\alpha + 1/L)^{-1}. \tag{2}$$

Y is the conventional photoelectron quantum yield of a thick homogeneous sample (e.g., head groups or tails only), α is the optical absorption coefficient, L is the electron attenuation length (electron mean free path), and d_0 defines a characteristic sample thickness from which approximately 63% (i.e., the fraction $1 - e^{-1}$) of the electrons originate. d_0 is a measure of the depth resolution in photoelectron microscopy; smaller values of d_0 permit higher resolution of surface detail. In principle there are two terms representing additive photoemission from the head groups and from the lipid tails. Thus, for the heads-down orientation

$$Y_d = Y[1 - e^{-d/d_0}]e^{-d'/d'_0} + Y'[1 - e^{-d'/d'_0}], \tag{3}$$

where d_0 is defined by Eq. 2 and the corresponding primed quantities refer to the lipid tails. Reflection effects and change-of-surface barrier effects have been neglected. Neglecting the photoemission from the lipid tails of Bchl *a* because of their relatively low quantum yields (i.e. $Y' \ll Y$) and also neglecting the optical absorption of the lipid tails, Eq. 3 reduced to

$$Y_d = Y[1 - e^{-d/d_0}]e^{-d'/L'}. \tag{4}$$

All of these quantities are of course excitation wavelength-dependent.

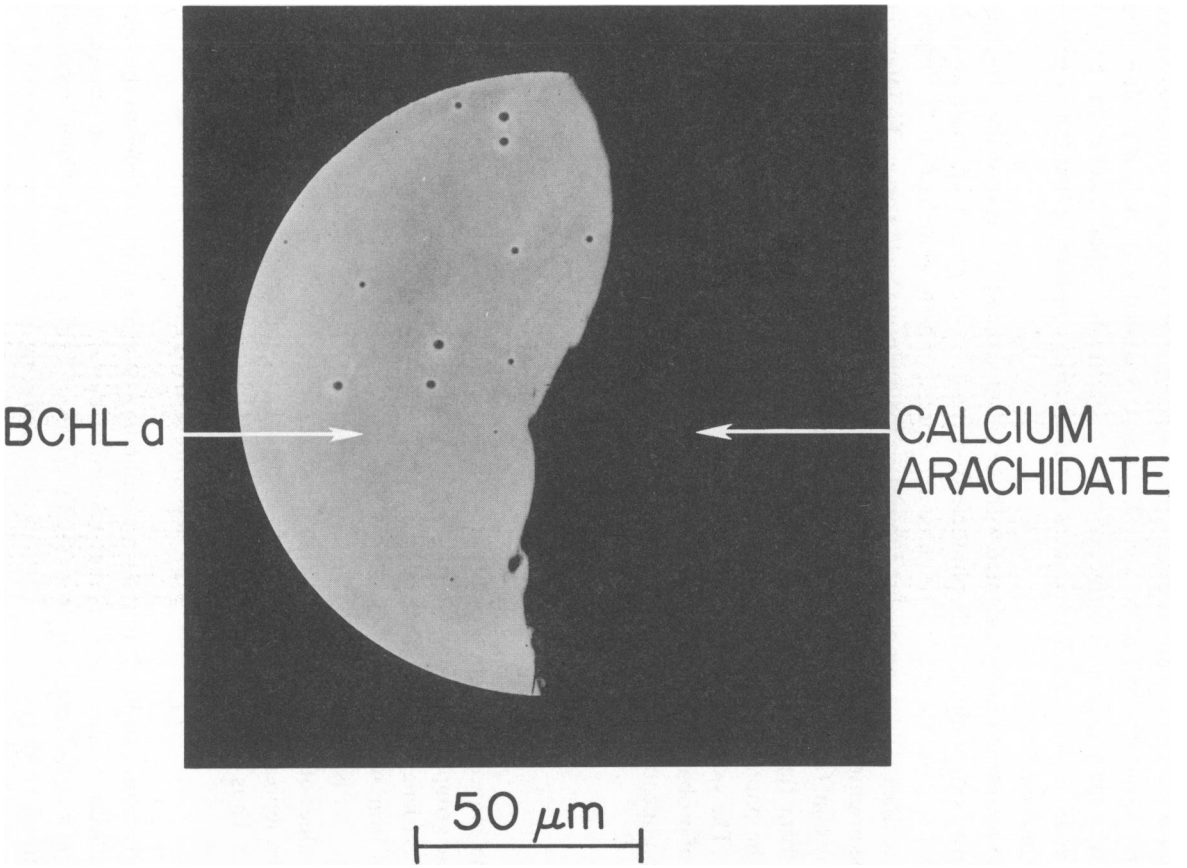

FIGURE 3 Photoelectron micrograph of one monolayer of Bchl *a* deposited on two monolayers of calcium arachidate. The negative was contact printed on the fiber optic window of the photoelectron microscope. Exposure time was 40 s.

Although accurate values for all the quantities in Eqs. 1–4 are not available, reasonable estimates can be made. The diameter of the tetrapyrrole nucleus is about 10 Å. At 220 nm, we take $\alpha \sim 10^{-3}$ Å^{-1} because this is on the order of α observed for the similar compounds Pc and protoporphyrin (Schechtman, 1968). The attenuation length should be about the same as for Pc since Bchl *a* and Pc not only have related structures, but exhibit very similar quantum yield curves. For Pc $L \sim 10$–15 Å (Pong and Smith, 1973; Burke et al., 1974). With these values, $L^{-1} \gg \alpha$, so that from Eq. 2, $d_0 \sim L$ and the exact value of α is not important. Summing terms for each layer with $d = 10$ Å and $L = 15$ Å, Eqs. 1 and 4 predict that about 90% of the total photoemission from an infinite stack of Bchl *a* bilayers arises from the top heads-up monolayer.

The relative brightness of the heads-up vs. heads-down monolayers is given by the attenuation factor $e^{-d'/L'}$ of Eq. 4. If we assume for simplicity an extended conformation of Bchl *a* perpendicular to the plane of the bilayer, d' is roughly the length of the hydrocarbon chain: $d' \sim 20$ Å. The value of L' depends on the kinetic energy of the electrons. It is probably somewhat greater than L for Pc. If $L' = 20$ Å, then the attenuation factor is simply $e^{-1} = 0.37$ and Eq. 4 predicts that the heads-up monolayer is about three times as bright as the heads-down monolayer, in agreement with the experimental data. This agreement may be partially fortuitous, because of the approximations in the calculation and the experimental uncertainty in the photoelectric measurements.

There is little reason to believe that the Bchl *a* is organized as pure bilayers in chromatophores of photosynthetic bacteria. It is more probable that the Bchl *a* exists as a complex with proteins imbedded in a dynamic lipid bilayer matrix (Clayton and Clayton, 1972). However, the Bchl *a* monolayer is a relevant model system having the correct thickness and asymmetry to test the ability of photoelectron microscopy to see Bchl *a* against a lipid background. The photoelectron micrograph of Fig. 3 shows that high contrast remains even when the sample thickness is reduced to one monolayer. The difference between the contrast of heads-up and heads-down monolayers shows that bilayer asymmetry can be detected by photoelectron microscopy. Taken together, these results indicate that it should be possible to utilize the photoemissive property of Bchl *a* to study the distribution and organization of photoreceptors in intact and freeze-fractured bacterial chromatophores.

We are pleased to acknowledge useful discussions with Drs. G. Bruce Birrell, Rudy J. Dam, Gertrude F. Rempfer, William Pong, and Ronald A. Powell. We wish to thank Keith F. Kongslie for expert technical assistance.

Support for this work was provided by National Science Foundation Grant PCM 76-22165. The photoelectron microscope was constructed under Public Health Service Grant CA 11695 from the National Cancer Institute.

Received for publication 29 August 1977.

REFERENCES

BLODGETT, K. B. 1935. Films built by depositing successive monomolecular layers on a solid surface. *J. Am. Chem. Soc.* **57**:1007.

BURKE, C. A., G. B. BIRRELL, G. H. LESCH, and O. H. GRIFFITH. 1974. Depth resolution in photoelectron microscopy of organic surfaces. The photoelectric effect of phthalocyanine thin films. *Photochem. Photobiol.* **19**:29.

CLAYTON, R. K., and B. J. CLAYTON. 1972. Relation between pigments and proteins in the photosynthetic membranes of *Rhodopseudomonas spheroides*. *Biochim. Biophys. Acta.* **283**:492.

DAM, R. J., and O. H. GRIFFITH. 1976. Photoelectron microscopy of biological surfaces. Excitation source brightness requirements. *Proc. Soc. Photo-Opt. Instrum. Eng.* **78**:143.

DAM, R. J., C. A. BURKE, and O. H. GRIFFITH. 1974*a*. Photoelectron quanum yields of the amino acids. *Biophys. J.* **14**:467.

DAM, R. J., K. F. KONGSLIE, and O. H. GRIFFITH. 1974*b*. The photoelectron quantum yields of hemin, hemoglobin, and apohemoglobin. Possible applications to photoelectron microscopy of heme proteins in biological membranes. *Biophys. J.* **14**:933.

DAM, R. J., K. F. KONGSLIE, and O. H. GRIFFITH. 1975. Photoelectron quantum yields and photoelectron microscopy of chlorophyll and chlorophyllin. *Photochem. Photobiol.* **22**:265.

GRIFFITH, O. H., and R. J. DAM. 1976. Photoelectron microscopy and quantum yields of membrane phospholipids. *Proc. Electron Microsc. Soc. Am.* **32**:33.

GRIFFITHS, M., and R. Y. STANIER. 1956. Some mutational changes in the photosynthetic pigment system of *Rhodopseudomonas spheroides*. *J. Gen. Microbiol.* **14**:698.

HOLT, A. S., and E. E. JACOBS. 1954. Spectroscopy of plant pigments. II. Methyl bacteriochlorophyllide and bacteriochlorophyll. *Am. J. Bot.* **41**:718.

KATZ, J. J., H. H. STRAIN, A. L. HARKNESS, M. H. STUDIER, W. A. SVEC, T. R. JANSON, and B. T. COPE. 1972. Esterifying alcohols in the chlorophylls of purple photosynthetic bacteria. A new chlorophyll, bacteriochlorophyll (gg), all-trans geranylgeranyl bacteriochlorophyllide *a*. *J. Am. Chem. Soc.* **94**:7938.

KIM, W. S. 1966. Complete fractionation of bacteriochlorophyll and its degradation products. *Biochim. Biophys. Acta.* **112**:392.

PONG, W., and J. A. SMITH. 1973. Photoelectric emission from copper phthalocyanine films. *J. Appl. Phys.* **44**:174.

SCHECHTMAN, B. H. 1968. Photoemission and optical studies of organic solids: phthalocyanines and porphyrins. Ph.D. thesis, Stanford Electronics Laboratories, Stanford University, Stanford, Calif.

SISTROM, W. R. 1966. The spectrum of bacteriochlorophyll in vivo: observations on mutants of *Rhodopseudomonas spheroides* unable to grow photosynthetically. *Photochem. Photobiol.* **5**:845.

SPERLING, W., and K. E. BACON. 1966. Chlorophyll monolayers and multilayers. I. Methods of preparation and spectroscopic characterization. *Photochem. Photobiol.* **5**:857.

SPICER, W. E. 1972. Photoelectric Emission in Optical Properties of Solids. North-Holland Publishing Co., Amsterdam. 758.

VERNON, L. P., and G. R. SEELY. 1966. The Chlorophylls. Academic Press, Inc., New York. 165.

WEIGL, J. W. 1953. Concerning the absorption spectrum of bacteriochlorophyll. *J. Am. Chem. Soc.* **75**:999.